Materials Science in Semiconductor Processing 27 (2014) 427–432

Contents lists available at ScienceDirect

Materials Science in Semiconductor Processing

journal homepage: www.elsevier.com/locate/mssp

A facile non-organometallic synthesis of hexadecylamine-capped ZnSe nanoparticles

Oluwatobi S. Oluwafemi [a,*], Vuyelwa Ncapayi [a], Oseyemi Olubomehin [b], Otolorin A. Osibote [c], Sandile P. Songca [d]

[a] Department of Chemistry, Cape-peninsula University of Technology, P. O Box 652 Capetown Campus, 8000 South Africa
[b] Department of Chemical Sciences, OlabisiOnabanjo University, P. O. Box 364, Ago-Iwoye, Ogun State, Nigeria
[c] Department of Physics, Cape-Peninsula University of Technology, P. O Box 652, Cape Town 8000, South Africa
[d] Department of Chemistry and Chemical Technology, Walter Sisulu University, Private bag X1, Mthatha 5117, South Africa

ARTICLE INFO

Available online 28 July 2014

Keywords:
Nanoparticles
ZnSe
Hexadecylamine
Quantum confinement
X-ray diffraction
Optical spectroscopy

ABSTRACT

The synthesis of hexadecylamine (HDA)-capped ZnSe nanoparticles via a facile method that is not mediated by organometallic compounds at low temperature is hereby reported. The synthesis involves the addition of an aqueous solution of zinc chloride to a selenide ion solution prepared by the reduction of selenium powder. By varying the reduction time, we studied the size, optical and structural properties of the as-synthesised nanoparticles. The as-synthesised ZnSe nanocrystals were characterised by UV–visible (UV–vis) absorption and PL spectroscopy, transmission electron microcopy (TEM), high-resolution transmission electron microscopy (HRTEM) and X-ray diffraction (XRD). All the particles exhibited strong quantum confinement in their optical properties with band-edge luminescence.

1. Introduction

Colloidal semiconductor nanocrystals (NCs) have attracted great attention due to their unique size-tunable optical and electronic properties as well as their potential applications in solar cells, light-emitting diodes (LEDs) and bio-labels. Among the A(II)B(VI) family of semiconductor nanocrystals [where A(II) is an element of group 12 and B(VI) an element of group 16 of the periodic table of elements], ZnSe is of special interest as it exhibits, via quantum confinement effects, tunable blue-ultraviolet (UV) luminescence. This UV range is practically difficult to obtain for cadmium-based systems such as CdSe, for which the toxicity of cadmium is an additional disadvantage [1,2]. ZnSe is an n-type and intrinsic direct band gap semiconductor with a wider band gap of 2.58 eV (480 nm) at 25 °C and transmittance range of 0.5–22 μm [3,4]. As an important semiconductor material of low toxicity when compared to CdSe, it is potentially a better material of choice for short-wavelength photoelectronic devices such as blue laser diodes, light-emitting diodes, photodetectors, biomedical labelling and sensors than other II–VI semiconductor materials [3–7]. It is also a promising candidate for the replacement of the toxic CdS in the buffer layer due to its wider band gap (2.58 eV) compared tothat of CdS (2.4 eV) [8] and useful in high resolution thermal imaging systems for correcting colour distortion, which is often inherent in other lenses used in the system [9,10].

Several methods have been reported for the synthesis of ZnSe nanoparticles. These are based mostly on the methods used to prepare CdSe nanoparticles by simply replacing the cadmium source with its zinc analogue. Hence, the method of preparation experienced limitations

* Corresponding author. Tel.: +27 765110322, +27 214603155.
E-mail address: oluwafemi.oluwatobi@gmail.com (O.S. Oluwafemi).

http://dx.doi.org/10.1016/j.mssp.2014.07.007
1369-8001/

like those for the preparation of CdSe nanoparticles. Similar to the cadmium analogue, the synthesis of ZnSe nanoparticles started with the use of arrested precipitation techniques. However, these earlier reports only provided optical absorption with no luminescence information [11]. The improved methods for the synthesis of ZnSe include the use of the supersaturated glass solution [12], sol–gel method [13], organometallic routes [14,15], solvothermal routes [16,17], single source precursor routes [18,19], metal organic chemical vapour deposition (MOCVD) [20], liquid–solid-solution processes [21], and hydrothermal methods [22]. Though well dispersed nanocrystals have been successfully prepared using these methods, these techniques are complicated and require expensive instruments, high operation temperatures, rigorous conditions and the use of pyrophoric, toxic organometallic compounds in the preparation of the selenide source. This limits the large-scale production and industrial applications of the material. In another development, Xiong et al., reported the synthesis of spherical cubic structure ZnSe nanoparticles using sodium selenosulphate as the selenium precursor [23]. However, the reaction required a longer time and the selenium precursor used was unstable at room temperature. Our group has also reported a simple and faster synthetic route for the synthesis of organic and water soluble CdSe nanoparticles using NaHSe as the selenium source and, hexadecylamine (HDA), tri-octyl phosphine oxide (TOPO), cysteine, starch and ascorbic acid as capping agents [24–27]. We have also extended this method to the synthesis of water soluble ZnSe using biopolymers as capping agents [28,29]. Furthermore, Dong et al., also reported the synthesis of highly luminescent water soluble ZnSe/ZnS core/shell quantum dots (QDs) in the blue region by a two-step method using NaHSe as the selenium source for the preparation of the oil soluble ZnSe core [30]. Previously, Zan and Ren used this selenium precursor for the synthesis of water soluble ZnSe(S) alloy under various synthetic conditions. They observed that the pH value of the Zn precursor solution and the molar ratio of Zn^{2+}: HSe^{-}: MPA had significant influence on the optical properties and the structure of the as-prepared ZnSe(S) QDs [31]. In a recent development, Florence et al., reported the synthesis of organic ligand capped nanoflakes and rod shaped ZnSe nanostructures using SeO_2 as the selenium source and, cetyltrimethylammonium bromide (CTAB) and 2-(N-salicylideneamino)-3-carboxyethyl-4, 5-dimethylthiophene [32,33] as the capping agents.

Alkylamines have been shown to improve the luminescence efficiency of quantum dots (QDs) by passivating the surface defects, behaving as non-radiative relaxation centres for the electron–hole recombination [34,35]. They behave as complex ligands for cadmium in the source solutions and as capping ligands on the surface of the QDs in the product colloidal solution. Among the alkylamines, primary amines have been shown to give high emission intensity due to their high electron donating ability, high capping density and small stereochemical interference [36]. In this paper, we report a simple, non-organometallic, low temperature and reproducible method for the synthesis of organically-capped ZnSe nanoparticles using hexadecylamine (long chain primary amine) as the capping agent and NaHSe as the selenium precursor. The reaction involves reduction of selenium powder in water to produce oxygen-free NaHSe as the selenium precursor followed by the addition of an aqueous solution of zinc chloride and thermolysis in hexadecylamine (HDA). By varying the reduction time for the synthesis of selenium precursor at room temperature, the temporal evolution of the size, optical and structural properties of the as synthesised nanoparticles was investigated. The nanoparticles were characterised by UV–vis absorption and photoluminescence (PL) spectroscopy, XRD and TEM.

2. Material and methods

2.1. Materials

Zinc chloride, sodium borohydride ($NaBH_4$), deionised water (HPLC grade), methanol, toluene, tri-*n*-octylphosphine (TOP), hexadecylamine (HDA), were purchased from Aldrich and the selenium powder from Merck. All the chemicals were of analytical grades and used as purchased.

2.2. Characterisation

A Perkin Elmer Lamda 20 UV–vis spectrophotometer was used to carry-out the absorption spectra in the 200–1100 nm wavelength range, while room temperature photoluminescence (PL) spectra were recorded on a Perkin Elmer LS 55 luminescence spectrometer. Samples were placed in quartz cuvettes (1 cm path length). XRD measurements of the samples were performed using a Bruker aXS D8 advanced diffractometer with Cu Kα radiation ($\lambda = 1.5406$ Å) operated at 40 kV and 40 mA. A JEOL 2100 TEM operating at 200 KV was used for TEM and HRTEM measurements while Image J software was used to calculate the particle size and size distribution.

2.3. Synthesis of HDA–capped ZnSe nanoparticles

In a typical room temperature reaction, 0.32 mmol of selenium powder was mixed with 20 mL of deionised water in a three-necked flask. $NaBH_4$ (0.81 mmol) was carefully added to this mixture under nitrogen flow to produce NaHSe. After 2 h, 0.32 mmol of $ZnCl_2$ dissolved in 20 mL of deionised water was added to the colourless selenium ion solution. The solution was stirred for 30 min followed by addition of excess methanol. The resultant solution was then centrifuged. The ZnSe produced was dispersed in 6 mL TOP and stirred continuously to form the TOP–ZnSe solution, which was then injected into 6 g hot HDA at 160 °C under nitrogen flow. A sudden decrease in temperature was observed upon rapid introduction of the reagent mixture. The temperature was then gradually raised and kept constant at 160 °C for 20 min. The growth process was stopped by the addition of excess anhydrous methanol to the reaction mixture. This resulted in the reversible flocculation of the nanoparticles. The flocculate was separated from the supernatant by centrifugation. Excess methanol was removed under vacuum and the resultant particles were dissolved in toluene to give a

solution of nanocrystallites for characterisation. The same procedure was repeated for the synthesis of ZnSe nanoparticles using NaHSe produced after 4 and 6 h reduction times.

3. Results and discussions

The reduction was monitored at 2, 4 and 6 h. Addition of the aqueous $ZnCl_2$solution to the freshly prepared colourless NaHSe resulted in a pale-yellow reaction mixture, which increased in colour intensity as the reduction time of the selenium powder increases. The reaction scheme is shown below.

$$4NaBH_4 + 2Se + 7H_2O \overset{2h,\ N_2,\ RT}{\rightarrow} 2NaHSe + Na_2B_4O_7 + 14H_2$$

$$NaHSe + ZnCl_2 \overset{N_2,RT}{\rightarrow} ZnSe + NaCl + HCl$$

$$ZnSe + TOP \overset{HDA,160\ ^{\circ}C}{\rightarrow} HDA - capped\ ZnSe$$

3.1. Optical analysis

Figs. 1 and 2 show the temporal evolution of the absorption and photo-luminescence spectra of the HDA-capped ZnSe nanoparticles synthesised at reduction time of 2, 4 and 6 h. The absorption band-edge and emission maxima of all the nanoparticles synthesised within these periods are blue-shifted from the bulk band gap (480 nm, 2.58 eV), clearly showing quantum confinement [37]. The absorption band-edge and emission maxima shift to higher band gap (lower wavelength) as the reduction time increase. This indicates an increase in particle size as the reduction time decreases. The as-synthesised material show sharp absorption edges and excitonic shoulders at 4 and 6 hrs (Fig. 1B and C), signifying monodispersed particles with focussed size distribution. The excitonic shoulder broadened as the reduction time decreases and disappeared at 2 h (Fig. 1A). The absence of the excitonic peak at 2 h might be attributed to weak confinement due to the presence of large particle size nanocrystals [38,39]. The absorption band-edges as-calculated using the direct

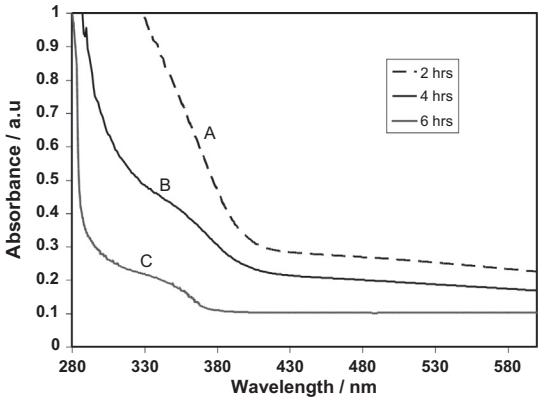

Fig. 1. Absorption spectra of ZnSe nanoparticles at reduction time of (A) 2, (B) 4 and (C) 6 h.

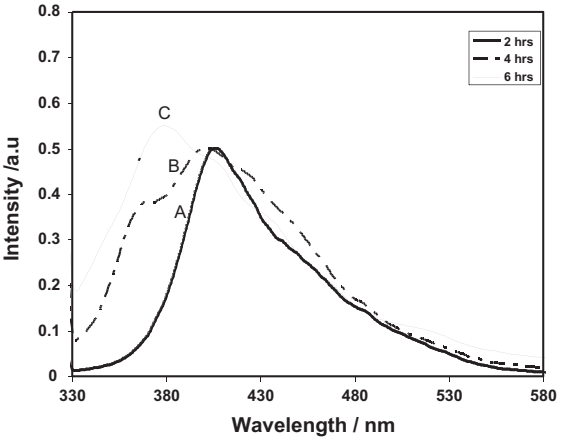

Fig. 2. Photoluminescence spectra (λ_{300} nm) of ZnSe nanoparticles at reduction time of (A) 2, (B) 4 and (C) 6 h.

band gap method [40] are 368 nm, 3.37 eV (6 h), 395 nm, 3.14 eV (4 h) and 401 nm, 3.09 eV (2 h) indicating increase in particle size as the reduction time decreased. This is contrary to the prediction from the colour of the solution after the addition of $ZnCl_2$ solution. The intensity of the pale yellow solution increased as the reduction time increases, signifying an increase in the particle size. We proposed that the large particles produced after the addition of $ZnCl_2$ at 6 and 4 hrs resulted in large nuclei (during nucleation) immediately after the injection into hot HDA. The presence of tailing band-edge in the optical spectrum at the beginning of the reaction (not shown here) confirmed this. As the reaction time increases these large nuclei are further nucleated and serve as a stable precursor for the formation of smaller nuclei. These smaller nanoparticles are slightly larger than the critical size of the monomer concentration and grow faster than the larger ones in the solution, due to their higher energy and lower stability hence narrowing of the size distribution [41]. The emergence of the excitonic shoulder and sharp absorption edge in the spectra at 6 and 4 hrs reduction timed further buttressed this. The PL spectra shown in Fig. 2A–C exhibit band-edge luminescence for excitation at 300 nm. The emission maxima are 381 nm, 3.25 eV (6 h); 402 nm, 3.08 eV (4 h) and 407 nm, 3.05 eV (2 h). The unevenness of the curves at 6 and 4 hrs reduction times is associated with the presence of structural defects like interstitials, selenium vacancies and dangling bond due to the smaller size of the nanoparticles [42]. As the particle size decreases, the surface to volume ratio increases thereby increasing the number of surface atoms and energy. This increases the density of the surface defects and thus, significantly affects the efficiency of the electronic passivation provided by the capping ligand [23,43].

3.2. Structural analysis

Fig. 3 shows the TEM images and size distributions of the ZnSe nanoparticles synthesised at the different reduction times. The images show well-defined, small,

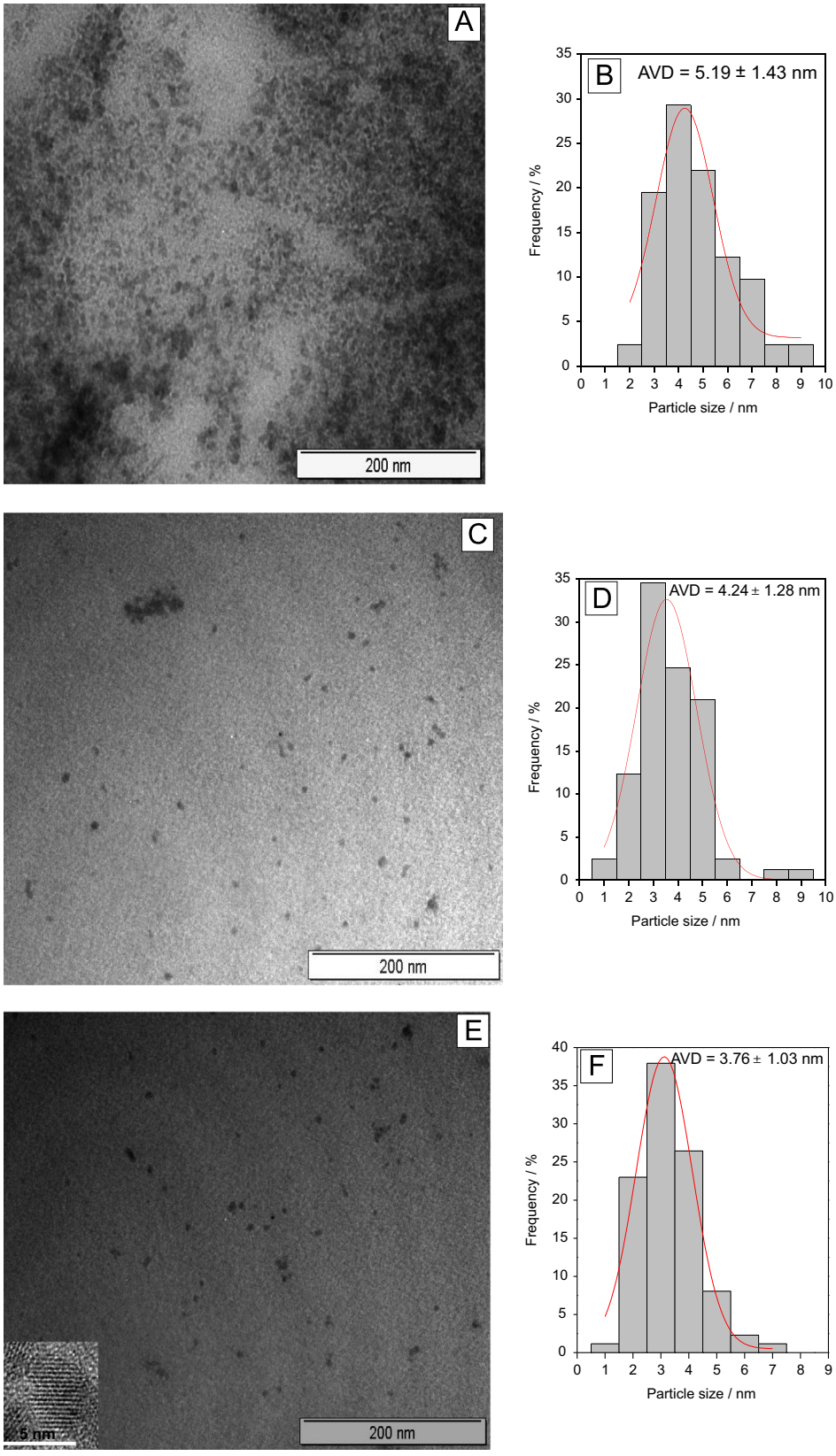

Fig. 3. TEM image (A) and particle size distribution (B) of ZnSe nanoparticles at reduction time of 2 h. (C) and particle size distribution (D) of ZnSe nanoparticles at reduction time of 4 h. (E) with single HRTEM image (inlet) and particle size distribution. (F) of ZnSe nanoparticles at reduction time of 6 h.

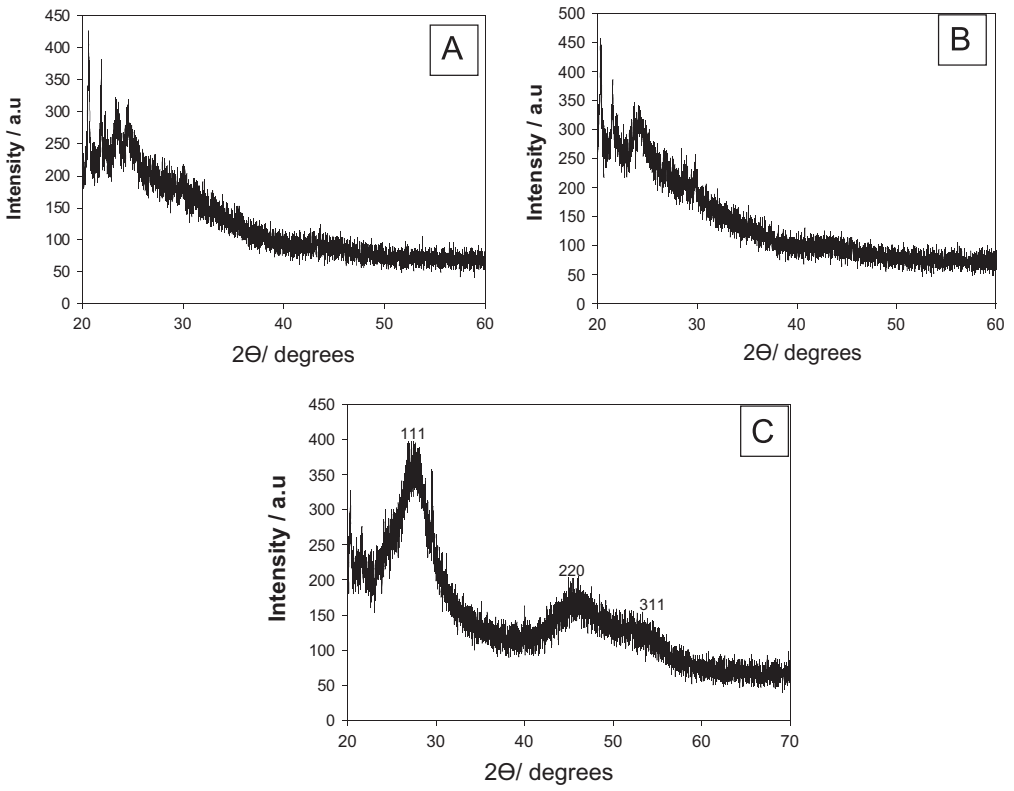

Fig. 4. XRD Pattern of ZnSe nanoparticles at reduction time of (A) 6, (B) 4 and (C) 2 h.

monodispersed and spherical particles at 4 and 6 h (Fig. 3C–F) and slightly larger particles at 2 h (Fig. 3A and B) which are very close to each other, appearing as aggregates. This further supports our proposition for the absence of the excitonic shoulder in the absorption spectrum at 2 h reduction time. The average particle sizes as determined from the TEM images are 3.76 ± 1.03 nm (6 h), 4.24 ± 1.28 nm (4 h) 5.19 ± 1.43 nm (2 h). The increase in the particle sizes as the reduction time decreases corresponds with the observed red-shift in the absorption spectrum. Fig. 3E (inset) shows the HRTEM image of a single ZnSe nanoparticle at 6 h reduction time. The existence of lattice planes in the HRTEM image confirms the crystallinity of the ZnSe nanocrystals. The measured lattice spacing (d) of 0. 278 nm correspond to the $d(200)$ plane of sphalerite cubic ZnSe. Fig. 4A–C show the wide angle X-ray diffraction patterns of the HDA-capped ZnSe nanocrystals. The broad nature of the XRD peaks is attributed to the nanocrystalline nature of the as-synthesised ZnSe nanoparticles, which is consistent with the results from the optical analysis. Due to the smaller particle size, the diffractograms at 6 and 4 h reduction times (Fig. 4B and C) show broad peaks from which a clear identification of either hexagonal or cubic phase is difficult. As the reduction time decreases, the crystallinity improves and the diffraction peaks become more clearly resolved (Fig. 4C). The XRD pattern at 2 h shows three diffraction peaks corresponding to the (111), (220) and (311) planes of sphalerite cubic ZnSe with a lattice constant of $a=5.667$, which is consistent with the JCPDS card number 80-0021 for cubic ZnSe. The clear and abundant (111) peak in Fig. 4C indicates the preferential growth of crystallites in this direction. The average crystal size as calculated based on the width of the peak due to (111) plane by using Scherrer's formula is 3.35 nm which is consistent with the TEM result.

4. Conclusion

We have successfully achieved the synthesis of HDA – capped ZnSe nanoparticles via a facile, non-organometallic compound mediated method at low temperature. By varying the reduction time of the selenium, we studied the size, optical and structural properties of the as-synthesised nanoparticles formed from the NaHSe produced. The results of the characterisation by UV–vis absorption and PL spectroscopy, XRD and TEM are presented and discussed. The temporal evolution of the absorption and photo-luminescence spectra of the as-synthesised nanoparticles indicate an increase in the absorption band-edge and emission maxima to higher band gap as the reduction time increases. This indicates that shorter reduction reaction time favoured the formation of larger particle size ZnSe NPs under this synthetic route. Furthermore, it should be noted that there is no definite advantage of one reduction time over another. The particle size of choice will determine the length of reduction time. Compared with the traditional methods this technique is simple, environmentally benign, inexpensive, involving the use of relatively non toxic reagent, short

reaction time and is promising for the large scale synthesis of high quality ZnSe nanoparticles for their industrial applications.

Acknowledgement

This work was supported by the National Research Foundation (NRF), South Africa. The authors thank Dr I.A Oluwafemi for technical assistance, Dr. Manfred Scriba (Council for Scientific and Industrial Research, CSIR, South Africa) for the microscopic measurement and Prof. Revaprasadu for the opportunity to do the preliminary work in his group.

References

[1] M.A. Haase, J. Qiu, J.M. Depuydt, H. Cheng, Appl. Phys. Lett. 58 (1991) 1272.
[2] H. Jeon, J. Ding, W. Patterson, A.V. Nurmiko, Appl. Phys. Lett. 59 (1991) 3619.
[3] A. Ennaoui, S. Siebntrit, M.C. Lux-Steiner, W. Riedl, F. Karg, Solar Energy Mater. Solar Cells 67 (2001) 31.
[4] K.R. Murali, K. Thilakvathy, S. Vasantha, R. Ooomen, Chalcogenide Lett. 5 (2008) 111.
[5] N. Kouklin, L. Menon, A.Z. Wong, D.W. Thompson, J.A. Woollam, P.F. Williams, Appl. Phys. Lett. 79 (2001) 4423.
[6] C.C. Kim, S. Sivananthan, Phys. Rev. B 53 (1996) 1475.
[7] G.F. Neumark, R.M. Park, J.M. Depuydt, Phys. Today 47 (1994) 26.
[8] C.D. Lokhande, P.S. Patil, H. Tributsch, A. Ennaousi, Solar Energy Mater. 55 (1998) 379.
[9] H. Luo, J.K. Furdyna, Semicond. Sci. Technol. 10 (1995) 1041.
[10] P. Qi, Y.J. Dong, Y.D. LiAngew, Chem. Int. Ed. 42 (2003) 3027.
[11] N. Chestnoy, R. Hull, L.E. Brus, J. Chem. Phys. 85 (1986) 2237.
[12] V.J. Leppert, S.H. Risbud, M.J. Fendorf, Philos. Mag. Lett. 75 (1997) 29.
[13] G. Li, M.J. Nogami, Appl. Phys. 75 (1994) 4276.
[14] M.A. Hines, P.J. Guyot-Sionnest, J. Phys. Chem. B 102 (1998) 3655.
[15] P. Reiss, G. Quemard, S. Carayon, S.J. Bluese, F. Chandezon, A. Pron, Mater. Chem. Phys 84 (2004) 10.
[16] W. Wang, Y. Geng, P. Yan, F. Liu, Y. Xie, Y. Qian, J. Am. Chem. Soc. 121 (1999) 4062.
[17] M.S. Selim, R. Seoudi, A.A. Shabaka, Mater. Lett. 59 (2005) 2650.
[18] N. Revaprasadu, M.A. Malik, P. O'Brien, M.M. Zulu, G. Wakefield, J. Mater. Chem. 8 (1988) 1885.
[19] M. Afzaal, D. Crouch, M.A. Malik, M. Motevalli, P. O'Brien, J.H. Park, J.D. Woollins, Eur. J. Inorg. Chem. 2004 (2004) 171.
[20] C.E.D. Bourrait, Appl. Phys. Lett. 68 (1996) 2418.
[21] X. Wang, J. Zhuang, Q. Peng, Y.D. Li, Nature 437 (2005) 121.
[22] Y. Jiao, D. Yu, Z. Wang, K. Tang, X. Sun, Mater. Lett. 61 (2007) 1541.
[23] S. Xiong, S. Huang, A. Tang, F. Teng, Mater. Lett. 61 (2007) 5091.
[24] O.S. Oluwafemi, N. Revaprasadu, New. J. Chem. 10 (2008) 1432.
[25] O.S. Oluwafemi, N. Revaprasadu, Physica B 404 (2009) 1204.
[26] O.S. Oluwafemi, Colloids Surf. B: Biointerface 73 (2009) 382.
[27] O.S. Oluwafemi, S.P. Songca, Mater. Lett. 75 (2012) 84.
[28] O.S. Oluwafemi, O.O. Adeyemi, Mater. Lett. 64 (2010) 2310.
[29] O.S. Oluwafemi, N. Revaprasadu, O.O. Adeyemi, Colloids Surf. B: Biointerface 79 (2010) 126.
[30] B. Dong, L. Cao, G. Su, W. Liu, Chem. Commun. 46 (2010) 7331.
[31] F. Zan, J. Ren, Luminescence 25 (2010) 378.
[32] S.S. Florence, J. Rita, A.D. Lawrence, M. Umadevi, Mater. Lett. 86 (2012) 129.
[33] S.S. Florence, M. Umadevi, J. Rita, A.D. Lawrence, Mater. Lett. 108 (2013) 5.
[34] L. Qu, X. Peng, J. Am. Chem. Soc. 124 (2002) 2049.
[35] D.V. Talapin, A.L. Rogach, A. Kornowski, M. Haase, H. Weller, Nano. Lett. 1 (2001) 207.
[36] K. Nose, H. Fujita, T. Omata, S.O.Y. Matsuo, H. Nakamura, H. Maeda, J. Lumin. 126 (2007) 21.
[37] L.E. Brus, J. Chem. Phys. 80 (1984) 4403.
[38] S.N. Sarangi, S.N. Sahu, Physica E23 (2004) 159.
[39] K. Yu, S. Singh, N. Patrito, V. Chu, Langmuir 20 (2004) 11161.
[40] J.L. Pankove, Optical Processes in Semiconductors, Dover Publications, New York, 1990.
[41] X. Peng, J. Wickham, A.P. Alivisatos, J. Am. Chem. Soc. 120 (1998) 5343.
[42] P.K. Sharma, R.K. Dutta, C.H. Liu, R. Pandey, A.C. Pandey, Mater. Lett. 64 (2010) 1183.
[43] L. Qu, X. Peng, J. Am. Chem. Soc. 124 (2002) 2049.